molecules

MDPI

Article

Regioisomers Salviprolin A and B, Unprecedented Rosmarinic Acid Conjugated Dinorditerpenoids from *Salvia przewalskii* Maxim

Xiangdong Su, Yichuang Wu, Meifang Wu, Jielang Lu, Shujie Jia, Xin He, Shuna Liu, Yuyang Zhou, Hui Xing and Yongbo Xue *

School of Pharmaceutical Sciences (Shenzhen), Sun Yat-sen University, Shenzhen 518107, China; suxd7@mail.sysu.edu.cn (X.S.); wuych39@mail2.sysu.edu.cn (Y.W.); wumf8@mail2.sysu.edu.cn (M.W.); lujlang@mail2.sysu.edu.cn (J.L.); jiashj@mail2.sysu.edu.cn (S.J.); hexin63@mail2.sysu.edu.cn (X.H.); liushn26@mail2.sysu.edu.cn (S.L.); zhouyy97@mail2.sysu.edu.cn (Y.Z.); xingh5@mail.sysu.edu.cn (H.X.)
* Correspondence: xueyb@mail.sysu.edu.cn

Abstract: *Salvia przewalskii* Maxim is a perennial plant from the genus *Salvia* (family Lamiaceae). The roots of *S. przewalskii* were long used as a traditional herb to treat blood circulation related illnesses in China. As part of our continuing interest in polycyclic natural products from medicinal plants, two unprecedented adducts comprised of a *dinor*-diterpenoid and a 9′-*nor*-rosmarinic acid derivative, linked by a 1,4-benzodioxane motif (**1** and **2**), were isolated from the roots of *S. przewalskii*. Their structures were established by extensive spectroscopic approaches including 1D, 2D NMR, and HRFABMS. Their cytotoxic activities against five human tumor cell lines were evaluated.

Keywords: *Salvia przewalskii* Maxim; Lamiaceae; dinorditerpenoids; rosmarinic acid; 1,4-benzodioxane

Citation: Su, X.; Wu, Y.; Wu, M.; Lu, J.; Jia, S.; He, X.; Liu, S.; Zhou, Y.; Xing, H.; Xue, Y. Regioisomers Salviprolin A and B, Unprecedented Rosmarinic Acid Conjugated Dinorditerpenoids from *Salvia przewalskii* Maxim. *Molecules* **2021**, *26*, 6955. https://doi.org/10.3390/molecules26226955

Academic Editor: Jorge A. R. Salvador

Received: 14 October 2021
Accepted: 11 November 2021
Published: 18 November 2021

1. Introduction

Salvia przewalskii Maxim is a perennial flowering herb which belongs to the genus *Salvia* (family Lamiaceae) [1]. This species is mainly distributed in regions of the Tibetan plateau, such as western parts of the Gansu and Sichuan provinces, as well as northwestern regions of the Yunnan province in China [2]. The roots of *S. przewalskii* were traditionally used as a folk medicine to achieve the therapeutic effects of enhancing blood circulation, remediating blood stasis, regulating menstruation, and relieving pain [3]. According to the Chinese Materia Medica, the roots of *S. przewalskii* were prescribed as a surrogate for Danshen (roots of *S. miltiorrhiza*), a well-known traditional Chinese medicine (TCM) used for the treatment of various cardiovascular diseases [4]. The secondary metabolites from *S. przewalskii* therefore attracted great interest towards their phytochemical investigation in recent decades. Intriguingly, abietane-type diterpenoids and phenolic acid derivatives are two major chemical constituents of the roots of *S. przewalskii*, which also appears in the phytological related *S. miltiorrhiza* [5–10]. Pharmacological studies revealed the beneficial effects of both the crude extracts and chemical constituents of *S. przewalskii*, including heart-protective, antioxidative, anti-inflammatory, antitussive, and antibacterial properties [4,11–14]. This research not only provided convincing evidence to support the traditional therapeutic effects of this species, but has also provided a comprehensive perspective of further potential medicinal applications.

1,4-Benzodioxane is a bicyclic scaffold which consists of a benzene-fused 1,4-dioxane. The versatile structural properties and potential therapeutic effects of this privileged heterocyclic scaffold have resulted in its incorporation in a number of drug design campaigns [15]. Natural products possessing this skeleton were discovered in several plant sources, for instance isoamericanoic acid B from *Acer tegmentosum*, and princepin from *Vitex glabrata* [16,17]. Studies illustrated that the biosynthetic origin of these bicyclic dimers

can be traced back to the oxidative dimerization of a number of small molecules, including phenylpropanoids, flavonoids, coumarins, and stilbenoids [18]. Moreover, naturally occurring chiral benzodioxanes demonstrated a range of therapeutic effects, including antiestrogenic, antimalarial, and anti-HCV activities [15].

In our continuing efforts to search for structurally unique and bioactive polycyclic natural products from medicinal plants [19–23], two undescribed phenylpropanoid-diterpenoid adducts (**1** and **2**) possessing a 1,4-benzodioxane scaffold, were encountered from the roots of *S. przewalskii*. Herein, we report the isolation, structural elucidation and evaluation of the cytotoxic effects of these compounds.

2. Results

A 70% aqueous acetone extract of the air-dried and powdered roots of *S. przewalskii* Maxim was partitioned between H_2O and $CHCl_3$. The $CHCl_3$ phase was subjected to repeated column chromatography, and then further purified by semipreparative HPLC to obtain compounds **1** and **2** (Figure 1). Their full structural elucidation was achieved after extensive spectroscopic analyses, including 1D and 2D NMR, and HRFABMS.

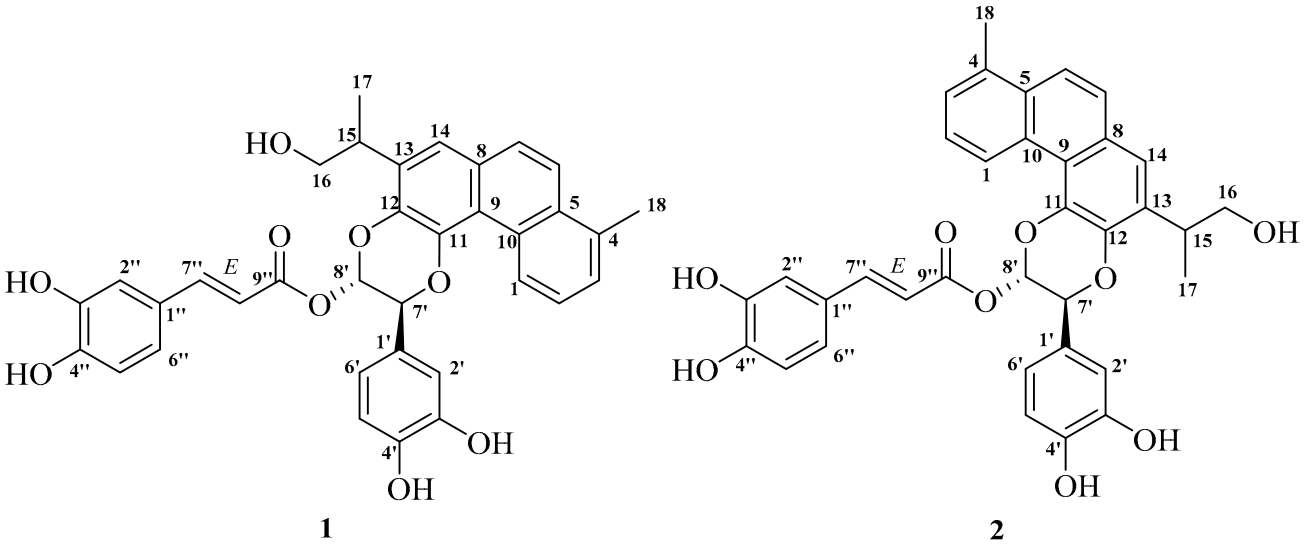

Figure 1. Structures of new compounds **1** and **2**.

Salviprolin A (**1**) was obtained as a dark brown solid. Its molecular formula was determined to be $C_{35}H_{30}O_9$ based on the deprotonated ion peak $[M - H]^-$ at *m/z* 593.1817 (calcd for $C_{35}H_{30}O_9$ 593.1812) in the HRFABMS (negative-ion mode) spectrum, indicating 21 degrees of unsaturation (Figure S1). The IR spectrum showed absorption bands characteristic of hydroxyl groups (3423 cm^{-1}), a carbonyl group (1703 cm^{-1}), aromatic rings (1601, 1521, and 1408 cm^{-1}) and ether groups (1284, 1252, and 1112 cm^{-1}) (Figure S2).

The ^{13}C NMR and DEPT spectra of **1** (Table 1, Figure S5) showed 35 carbon signals, including one ester carbonyl (δ_C 165.9), 14 quaternary C-atoms (eight aromatic carbons at δ_C 134.6, 132.2, 129.3, 120.3, 130.6, 134.2, 128.5, and 127.1, and six oxygenated aromatic carbons at δ_C 141.3, 138.3, 146.2, 146.3, 146.5, and 149.4), 17 methine groups (12 aromatic methines at δ_C 127.4, 126,4, 128.1, 122.4, 127.9, 120.9, 114.8, 116.2, 119.5, 115.5, 116.4, and 123.0, two olefinic methines at δ_C 148.0 and 114.0 and three aliphatic methines including two oxygenated carbons at δ_C 36.6, 76.0, and 90.4), one oxygenated methylene (δ_C 67.0) and two methyl groups (δ_C 17.1 and 20.5).

Table 1. ^{1}H (400 MHz) and ^{13}C (100 MHz) NMR data, and HMBC correlations for **1** [a] and **2** [a].

No	**1**			**2**		
	δ_C	δ_H **(Mult, *J*, Hz)**	**HMBC**	δ_C	δ_H **(Mult, *J*, Hz)**	**HMBC**
1	127.4	9.61 m	3, 5, 9	127.3	9.44 m	3, 5, 9
2	126.4	7.43 [c]	4, 10	126.3	7.40 [c]	4, 10
3	128.1	7.43 [c]	1, 4, 5, 18	128.1	7.40 [c]	1, 4, 5, 18
4	134.6	-		134.5	-	
5	132.2	-		132.2	-	
6	122.4	7.90 d (9.2)	4, 8, 10	122.1	7.85 d (9.1)	4, 8, 10
7	127.9	7.77 d (9.2)	5, 6, 8, 9, 14	127.7	7.75 d (9.1)	5, 8, 9, 14
8	129.3	-		128.9	-	
9	120.3	-		120.5	-	
10	130.6	-		130.3	-	
11	141.3	-		139.1	-	
12	138.3	-		140.4	-	
13	134.2	-		134.0	-	
14	120.9	7.51 s	7, 9, 12, 15	121.4	7.56 s	7, 9, 12, 15
15	36.6	3.42 m	12, 13, 14, 16, 17	36.5	3.57 m	12, 14, 16, 17
16	67.0	3.65 dd (10.4, 7.2) 3.85 dd (10.4, 5.6)	13, 15, 17	67.1	3.70 dd (10.4, 7.2) 3.92 dd (10.4, 5.6)	13, 15, 17
17	17.1	1.35 d (5.6)	13, 15, 16	17.3	1.42 d (6.8)	13, 15, 16
18	20.5	2.73 s	3, 4, 5	20.5	2.69 s	3, 4, 5
1′	128.5	-		128.6	-	
2′	114.8	7.12 d (1.9)	1′, 3′, 4′, 6′, 7′	114.9	7.11 br s	4′, 6′
3′	146.2 [b]	-		146.1 [b]	-	
4′	146.3 [b]	-		146.4 [b]	-	
5′	116.2 [b]	6.84 [c] d (8.0)	1′, 3′, 4′, 6′	116.1 [b]	6.85 [c]	1′, 3′
6′	119.5	6.99 dd (8.0, 1.9)	1′, 2′, 4′, 7′	119.7	6.97 d (7.8)	2′, 4′, 5′, 7′
7′	76.0	5.52 d (3.8)	1′, 2′, 6′, 8′, 11	76.1	5.36 d (4.1)	1′, 2′, 6′, 8′, 12
8′	90.4	6.77 d (3.8)	1′, 7′, 9″, 12	90.8	6.74 d (4.1)	1′, 7′, 9″, 11
1″	127.1	-		127.0	-	
2″	115.5	7.16 d (1.5)	4″, 6″, 7″	115.5	7.17 br s	4″, 6″
3″	146.5	-		146.6 [b]	-	
4″	149.4	-		149.4	-	
5″	116.4 [b]	6.84 [c] d (8.0)	1″, 3″, 4″, 6″	116.4 [b]	6.85 [c]	1″, 3″, 4″, 6″
6″	123.0	7.04 dd (8.0, 1.5)	2″, 4″, 7″	123.0	7.02 d (7.8)	2″, 4″, 5″
7″	148.0	7.64 d (15.8)	1″, 2″, 6″, 9″	148.2	7.64 d (15.8)	1″, 2″, 6″, 9″
8″	114.0	6.29 d (15.8)	1″, 7″, 9″	113.8	6.30 d (15.8)	1″, 9″
9″	165.9	-		165.9	-	

[a] NMR data were recorded in acetone-d_6; [b] assignments may be interchanged; [c] overlapped peaks.

The ^{1}H NMR spectrum of **1** displayed a set of signals consistent with a 1,2,3-trisubstituted phenyl core [δ_H 9.61 (1H, m, H-1), 7.43 (2H, overlapping, H-2 and H-3)], a 1,2,3,4-tetrasubstituted phenyl ring [δ_H 7.90 (1H, d, J = 9.2 Hz, H-6) and 7.77 (1H, d, J = 9.2 Hz, H-7)], and a singlet aromatic proton [δ_H 7.51 (1H, s, H-14)] (Table 1, Figure S4). In the ^{1}H-^{1}H COSY spectrum (Figures 2 and S6), a spin-coupling system connecting an oxygenated methylene [H-16 (δ_H 3.65 and 3.85)] to a methine [H-15 (δ_H 3.42)], and continuing to a methyl group [H-17 (δ_H 1.35)], established the 1-isopropanol segment of CH_2(16)-CH(15)-CH_3(17). Since the 1D-NMR data of **1** were indicative of a highly oxygenated polycyclic structure unlike all previously known diterpenoids isolated from the *salvia* genus, a comprehensive analysis of its 2D-NMR spectroscopic data was conducted.

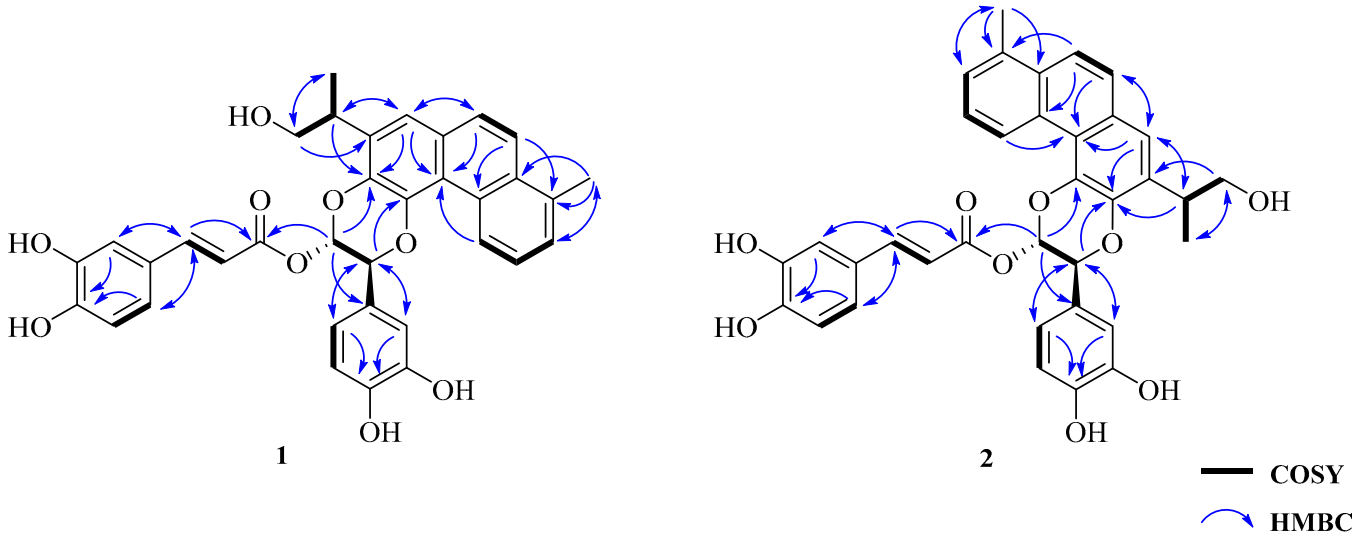

Figure 2. Key COSY and key HMBC correlations of compounds **1** and **2**.

The HMBC correlations from H-15 (δ_H 3.42) to C-12 (δ_C 138.3)/C-14 (δ_C 120.9), from H-14 to C-15 (δ_C 36.6), together with the HMBC correlations from H-16 (δ_H 3.65 and 3.85)/H-17 (δ_H 1.35) to C-13 (δ_C 134.2) confirmed the C-C linkage of C-15 to C-13 (Figures 2 and S7). Moreover, the HMBC correlations from H-18 (δ_H 2.73) to C-3 (δ_C 128.1)/C-5 (δ_C 132.2) were employed to locate a methyl group at C-4 (Figures 2 and S7). This led us to deduce the presence of a dinorditerpenoid residue, a structural motif which was observed in *R*-(+)-salmiltiorin E [24].

The additional ^{1}H NMR data demonstrated a 1,3,4-trisubstituted phenyl ring [δ_H 7.12 (1H, d, J = 1.9 Hz, H-2′), 6.84 (1H, d, J = 8.0 Hz, H-5′), 6.99 (1H, dd, J = 1.9, 8.0 Hz, H-6′)] skeleton typical of a caffeoyl moiety [δ_H 7.16 (1H, d, J = 1.5 Hz, H-2″), 6.84 (1H, d, J = 8.0 Hz, H-5″), 7.04 (1H, dd, J = 1.5, 8.0 Hz, H-6″), 7.64 (1H, d, J = 15.8 Hz, H-7″), 6.29 (1H, d, J = 15.8 Hz, H-8″)] (Table 1, Figure S4) [25]. In addition, the *trans*-coupled H-7″ and H-8″ were elucidated on the basis of their relatively large coupling constants (J = 15.8 Hz). The HMBC spectrum of **1** revealed HMBC correlations from H-7′ (δ_H 5.52) to C-11 (δ_C 141.3), and from H-8′ (δ_H 6.77) to C-12 (δ_C 138.3). Taken together with the ^{1}H-^{1}H COSY correlation between H-7′ and H-8′, this established the coexistence of two ether linkages of CH(7′)-*O*-C(11) and CH(8′)-*O*-C(12), ultimately suggesting the diterpenoid was fused at C-11 and C-12 by the aforementioned phenyl-1,4-benzodioxane moiety (Figures 2 and S7). The subsequent key HMBC correlations from H-7′ (δ_H 5.52) to C-2′ (δ_C 114.8), C-6′ (δ_C 119.5) and the HMBC interactions from H-2′ (δ_H 7.12)/H-6′ (δ_H 6.99) to C-7′ (δ_C 76.0) indicated the 1,3,4-trisubstituted phenyl ring was attached to the phenyl-1,4-benzodioxane moiety at C-7′ (Figures 2 and S7). Likewise, key HMBC correlations from H-8′ (δ_H 6.77) to C-9″ (δ_C 165.9) and C-1′ (δ_C 128.5) supported the conclusion that the *trans*-caffeoyl residue was linked to the phenyl-1,4-benzodioxane moiety at C-8′ by an ester group. Hence, the planar structure of **1** was determined as shown (Figure 2). Furthermore, the coupling constant between H-7′ and H-8′ (J = 3.8 Hz) was very close to that of H-7″ and H-8″ (J = 3.3 Hz) (i.e., similar to that of an oxidized isoamericanol A), and a ROE correlation between H-8′ and H-6′ as shown (Figures 3 and S9) suggesting the two protons at C-7′ and C-8′ to be *trans*-oriented. It was based on these that the 7′*R**, 8′*S**-configuration of **1** was provisionally assigned [26–28]. Consequently, the three-dimensional structure of **1** was determined as shown (Figure 1), and salviprolin A was assigned.

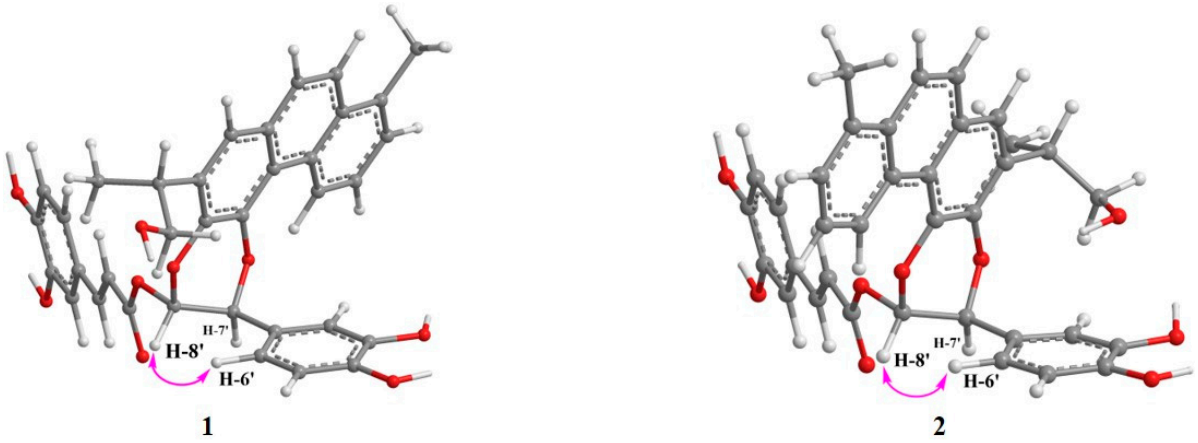

Figure 3. Energy-minimized structures of compounds **1** and **2** with Key ROE correlations.

Compound **2** was obtained as a dark brown solid, which had the same molecular formula as **1**, $C_{35}H_{30}O_9$, as deduced from a quasi-molecular ion peak in its HR-FAB-MS spectrum (Figure S12). The ^{1}H and ^{13}C NMR spectroscopic data of **2** were almost identical to those of **1** (Table 1, Figures S13 and S14), which suggested a large degree of structural similarity between the two compounds. Key HMBC correlations observed in the HMBC spectrum from H-7′ (δ_H 5.36) to C-12 (δ_C 140.4) and H-8′ (δ_H 6.74) to C-11 (δ_C 139.1), indicated the presence of an ether-linkage from C-12 to C-7′ and from C-11 to C-8′, respectively, instead of CH(7′)-*O*-C(11) and CH(8′)-*O*-C(12) as displayed in **1** (Figure S16). Thus, compound **2** was determined to be a regioisomer of **1** at the C-7′ and C-8′ positions. The ROE correlation between H-8′ and H-6′ suggested H-7′ and H-8′ to be *trans*-oriented as shown (Figures 3 and S18). Moreover, the coupling constant between H-7′ and H-8′ of **2** was almost identical to those of **1**, thereby indicating a 7′*R**, 8′*S**-configuration of **2**. The structure of compound **2** was therefore determined as shown (Figure 1) and named salviprolin B.

Compounds **1** and **2** were evaluated for in vitro cytotoxicity against the human tumor cell lines HL-60, SMMC-7721, A-549, MCF-7, and SW480 cell lines using the MTT method as previously reported [29]. *cis*-Platin (Sigma) was used as the positive control. Unfortunately, both compounds were found to be inactive with IC_{50} values of >40 μM (Table 2).

Table 2. Cytotoxic activity of compounds **1** and **2** [a].

Compound	A-549	HL-60	MCF-7	SMMC-7721	SW-480
1	>40	>40	>40	>40	>40
2	>40	>40	>40	>40	>40
cis-platin	15.6	0.9	14.9	13.8	19.1

[a] Results are expressed as IC_{50} values in μM; data were obtained from triplicate experiments; *cis*-platin was used as a positive control.

3. Discussion

Origanum dictamnus L. (family Lamiaceae) was previously reported to produce a series of benzodioxane-containing metabolites, for example, salvianolic acid P [30]. Interestingly, our current work on *S. przewalskii* from the Lamiaceae family also resulted in characterization of two unique *nor*-phenylpropanoid and *dinor*-diterpenoid adducts (**1** and **2**) containing a 1,4-benzodioxane nucleus. The above findings may suggest a similar biosynthetic pathway between these two species of the Lamiaceae family. To the best of our knowledge, this is the first report of natural chiral 1,4-benzodioxane adducts containing a *nor*-rosmarinic acid derivative and a *dinor*-diterpenoid. Derivatives of rosmarinic acid such as salvianolic acid, and dinorditerpenoids astanshinones are widely distributed in species from the Lamiaceae family, especially in the genus *Salvia* [31,32]. As with many constituents of *S. przewalskii* and *S. miltiorrhiza*, rosmarinic acid derivatives and dinorditer-

penoids also exhibit a wide range of therapeutic benefits, including anti-tumor, antioxidant, anti-inflammatory, and antibacterial properties [31–33]. Unfortunately, due to poor isolation yields, the biological evaluation of compounds **1** and **2** in this study was limited to a preliminary investigation into their cytotoxic activity. The privileged nature of their unique 1,4-benzodioxane motifs that feature both a hydrophilic phenolic moiety and a lipophilic diterpenoid, however, hold great potential for promising bioactivity in other therapeutic contexts. It is our hope that either improvement and scale-up of the isolation methods or a total synthesis approach will be able to provide quantities of **1** and **2** enough to facilitate their further pharmacological evaluation.

4. Experimental

4.1. General Experimental Procedures

Optical rotations were measured with a Horiba SEPA-300 polarimeter. UV spectra were recorded using a Shimadzu UV-2401A spectrophotometer equipped with a DAD and a 1 cm pathlength cell. Methanolic samples were scanned from 190 to 400 nm in 1 nm steps. IR spectra were obtained using a Tenor 27 spectrophotometer with KBr pellets. 1D and 2D NMR spectra were acquired on a Bruker DRX-500 spectrometer with TMS as internal standard. Chemical shifts (δ) were expressed in ppm with reference to the solvent signals. Mass spectra were recorded on a VG Auto Spec-3000 instrument or an API QSTAR Pulsar 1 spectrometer. Semipreparative HPLC was performed on an Agilent 1100 apparatus equipped with a UV detector and a Zorbax SB-C-18 (Agilent, 9.4 mm × 25 cm) column. Column chromatography was performed using silica gel (200–300 mesh and H, Qingdao Marine Chemical Co. Ltd., Qingdao, China), RP-18 gel (40–63 μm, Merck, Darmstadt, Germany), and MCI gel (75–150 μm; Mitsubishi Chemical Corporation, Japan). Fractions were monitored by TLC (GF254, Qingdao Marine Chemical Co. Ltd., Qingdao, China), and spots were visualized by heating silica gel plates sprayed with 10% H_2SO_4 in EtOH. All solvents were distilled prior to use.

4.2. Plant Materials

The air-dried and powdered roots of *S. przewalskii* Maxim (7.0 kg) were collected at Zhongdian County, Yunnan province, People's Republic of China, on August 2005, and the plant was identified by Prof. Xiao Cheng at Kunming Institute of Botany, Chinese Academy of Sciences. A specimen (No. 20050623 L2) was deposited in Kunming Institute of Botany, Chinese Academy of Sciences.

4.3. Extraction and Isolation

The air-dried and powdered roots of *S. przewalskii* Maxim (7.0 kg) were extracted with 70% aqueous acetone (24 h × 3 times) at room temperature and concentrated in vacuo to give a crude extract (1.3 kg). The extract was suspended in H_2O, and then extracted with $CHCl_3$. The $CHCl_3$-soluble extract (220.0 g) was chromatographed over a silica gel chromatography column (CC) (petroleum ether/acetone from 1:0 to 0:1) to give fractions SI–VII. Fr. SI was subjected to silica gel CC (petroleum ether/EtOAc from 20:1 to 0:1) to afford six subfractions (SI1–SI6). Fr. SI3 (647.0 mg) was subjected to Sephadex LH-20 gel CC ($CHCl_3$/MeOH, 1:1) to give four subfractions (SI3A–SI3D). Fr. SI3C was purified by silica gel CC (petroleum ether/$CHCl_3$/EtOAc, 70:28:2) to yield seven subfractions (SI3C1–SI3C7). Fr. SIII (6.3 g) was chromatographed over silica gel CC (petroleum ether/EtOAc, 16:1–2:3) to afford eight subfractions (SIII1–III8). Fr. SIII5 (648.0 mg) was purified by semipreparative HPLC (MeOH/H_2O, 85:15) to yield compounds **1** (3.2 mg) and **2** (4.0 mg).

*4.4. Salviprolin A (**1**)*

Dark brown solid; $[\alpha]_D^{26.2}$: −69.8° (*c* 1.21, MeOH); UV (MeOH) λ_{max} (log ε) 363 (2.2), 281 (2.4), 258 (2.7), 212 (2.8); IR (KBr) ν_{max} 3423, 2956, 1703, 1601, 1521, 1408, 1284, 1252, 1112, 804, 762 cm^{-1}; ^1H NMR and ^{13}C NMR see Table 1; negative FABMS *m/z* 593 ($[M - H]^-$; negative HRFABMS *m/z* 593.1817 (calcd. for $C_{35}H_{29}O_9$, 593.1812).

4.5. Salviprolin B (**2**)

Dark brown solid; $[\alpha]_D^{26.2}$: −204.2° (*c* 0.48, MeOH); UV (MeOH) λ_{max} (log ε) 364 (2.6), 281 (2.8), 258 (3.1), 209 (3.1); IR (KBr) ν_{max} 3431, 2959, 1703, 1608, 1523, 1383, 1285, 1200, 980, 763 cm^{-1}; ^1H NMR and ^{13}C NMR see Table 1; negative FABMS *m/z* 593 ($[M - H]^-$; negative HRFABMS *m/z* 593.1804 (calcd. for $C_{35}H_{29}O_9$, 593.1812).

4.6. Cytotoxic Assays

Colorimetric assays were performed to evaluate compound activity [29]. The following human tumor cell lines were used: the A549 lung cancer cell line, the HL-60 human myeloid leukemia cell line, the MCF-7 breast cancer cell line, the SMMC-7721 human hepatocarcinoma cell line, and the SW-480 human pancreatic carcinoma. All cells were cultured in RPMI-1640 or DMEM medium (Hyclone, Logan, UT, USA), supplemented with 10% fetal bovine serum (Hyclone) at 37 °C in a humidified atmosphere with 5% CO_2. Cell viability was assessed by conducting colorimetric measurements of the amount of insoluble formazan formed in living cells based on the reduction of 3-(4,5-dimethylthiazol-2-yl)-2,5-diphenyltetrazolium bromide (MTT) (Sigma, St. Louis, MO, USA). Briefly, 100 µL adherent cells were seeded into each well of a 96-well cell culture plate and allowed to adhere for 12 h before compound addition, while suspended cells were seeded just before compound addition, both with initial density of 1 × 105 cells/mL in 100 µL of medium. Each tumor cell line was exposed to the test compound at various concentrations in triplicate for 48 h, with *cis*-Platin (Sigma) as positive control. After incubation, MTT (100 µg) was added to each well, and the incubation was continued for 4 h at 37 °C. The cells were lysed with 100 µL of 20% SDS-50% DMF after removal of 100 µL of medium. The optical density of the lysate was measured at 595 nm in a 96-well microtiter plate reader (Bio-Rad 680). The IC_{50} value of each compound was calculated by Reed and Muench's method.

Supplementary Materials: The following are available online. The HR-FAB-MS, IR, UV and 1D, 2D NMR spectra of compounds **1** and **2** are available in supplementary materials. Figure S1: HRFABMS spectrum of **1**, Figure S2: IR spectrum of **1** (KBr), Figure S3: UV spectrum of **1** (MeOH), Figure S4: ^1H NMR spectrum of **1** in acetone-d_6, Figure S5: ^{13}C NMR spectrum of **1** in acetone-d_6, Figure S6: COSY spectrum of **1** in acetone-d_6, Figure S7: HMBC spectrum of **1** in acetone-d_6, Figure S8: HSQC spectrum of **1** in acetone-d_6, Figure S9: ROESY spectrum of **1** in acetone-d_6, Figure S10: UV spectrum of **2** (MeOH), Figure S11: IR spectrum of **2** (KBr), Figure S12: HRFABMS spectrum of **2,** Figure S13: ^1H NMR spectrum of **2** in acetone-d_6, Figure S14: ^{13}C NMR spectrum of **2** in acetone-d_6, Figure S15: HSQC spectrum of **2** in acetone-d_6, Figure S16: HMBC spectrum of **2** in acetone-d_6, Figure S17: COSY spectrum of **2** in acetone-d_6, Figure S18: ROESY spectrum of **2** in acetone-d_6.

Author Contributions: Conceptualization, Y.X. and X.S.; methodology, X.S. and Y.W.; formal analysis, M.W., J.L. and S.J.; investigation, X.H., S.L. and Y.Z.; writing, X.S. and Y.X.; supervision, Y.X. and H.X.; funding acquisition, Y.X., X.S. and H.X. All authors have read and agreed to the published version of the manuscript.

Funding: This research was financially supported by the National Natural Science Foundation of China (No. 21977120), the Key Basic Research Programme of the Science, Technology and Innovation Commission of Shenzhen (JCYJ20200109142215045), the Hundred Talents Program of Sun Yat-sen University (No. 75110-18841218), the China Postdoctoral Science Foundation (2020M673027 and 2019M663327), and the Fundamental Research Funds for the Central Universities of China (No. 75110-31610023).

Institutional Review Board Statement: Not applicable.

Informed Consent Statement: Not applicable.

Data Availability Statement: Supporting Information data include HRFABMS, IR, UV and 1D, 2D NMR spectral charts.

Acknowledgments: The authors would like to express deep gratitude to Shengxiong Huang from Kunming Institute of Botany, Chinese Academy of Sciences, for his valuable discussion about the structure elucidation.

Conflicts of Interest: The authors declare no conflict of interest.

Sample Availability: Samples of the compounds **1** and **2** are available from the authors.

References

1. Wang, N.; Niwa, M.; Luo, H.-W. Triterpenoids from *Salvia przewalskii*. *Phytochemistry* **1988**, *27*, 299–301. [CrossRef]
2. Liu, J.-M.; Nan, P.; Tsering, Q.; Tsering, T.-S.; Bai, Z.-K.; Wang, L.; Liu, Z.-J.; Zhong, Y. Volatile constituents of the leaves and flowers of *Salvia przewalskii* Maxim. from Tibet. *Flavour Fragr. J.* **2006**, *21*, 421–438. [CrossRef]
3. Wang, L.; Jiang, Y.-Y.; Zhang, L.; Wang, T.; Zhou, Y.-H. High-performance liquid chromatography fingerprints and simultaneous quantification of bioactive compounds in *Salvia przewalskii* Maxim. *Acta Chromatogr.* **2017**, *29*, 291–308. [CrossRef]
4. Wang, Y.-F.; Duo, D.-L.; Yan, Y.-J.; He, R.-Y.; Wu, X.-N. Bioactive constituents of *Salvia przewalskii* and the molecular mechanism of its antihypoxia effects determined using quantitative proteomics. *Pharm. Biol.* **2020**, *58*, 469–477. [CrossRef] [PubMed]
5. Wang, M.-M.; Dai, H.-X.; Li, X.-R.; Li, Y.-H.; Wang, L.-J.; Xue, M. Structural elucidation of metabolites of tanshinone I and its analogue dihydrotanshinone I in rats by HPLC–ESI-MS^n. *J. Chromatogr. B* **2010**, *878*, 915–924. [CrossRef]
6. Li, J.; Li, B.; Luo, L.; Cao, F.-L.; Yang, B.-Y.; Gao, J.; Yan, Y.-G.; Zhang, G.; Peng, L.; Hu, B.-X. Increased phenolic acid and tanshinone production and transcriptional responses of biosynthetic genes in hairy root cultures of *Salvia przewalskii* Maxim. treated with methyl jasmonate and salicylic acid. *Mol. Biol. Rep.* **2020**, *47*, 8565–8578. [CrossRef] [PubMed]
7. Ożarowski, M.; Piasecka, A.; Gryszczyńska, A.; Sawikowska, A.; Opala, A.P.B.; Mikołajczak, P.; Kujawski, R.; Kachlicki, P.; Buchwald, W.; Mrozikiewicz, A.S. Determination of phenolic compounds and diterpenes in roots of *Salvia miltiorrhiza* and *Salvia przewalskii* by two LC–MS tools: Multi-stage and high resolution tandem mass spectrometry with assessment of antioxidant capacity. *Phytochem. Lett.* **2017**, *20*, 331–338. [CrossRef]
8. Xu, G.; Yang, X.-W.; Wu, C.-Y.; Li, X.-N.; Zhao, Q.-S. Przewalskone: A cytotoxic adduct of a danshenol type terpenoid and an icetexane diterpenoid via hetero-Diels–Alder reaction from *Salvia przewalskii*. *Chem. Commun.* **2012**, *48*, 4438–4440. [CrossRef] [PubMed]
9. Xu, G.; Hou, A.-J.; Wang, R.-R.; Liang, G.-Y.; Zheng, Y.-T.; Liu, Z.-Y.; Li, X.-L.; Zhao, Y.; Huang, S.-X.; Peng, L.-Y.; et al. Przewalskin A: A New C23 Terpenoid with a 6/6/7 Carbon Ring Skeleton from *Salvia przewalskii* Maxim. *Org. Lett.* **2006**, *8*, 4453–4456. [CrossRef] [PubMed]
10. Xu, G.; Hou, A.-J.; Zheng, Y.-T.; Zhao, Y.; Li, X.-L.; Peng, L.-Y.; Zhao, Q.-S. Przewalskin B, a Novel Diterpenoid with an Unprecedented Skeleton from *Salvia przewalskii* Maxim. *Org. Lett.* **2006**, *9*, 291–293. [CrossRef]
11. Wang, Y.-F.; Duo, D.-L.; Yan, Y.-J.; He, R.-Y.; Wu, X.-N. Extract of *Salvia przewalskii* Repair Tissue Damage in Chronic Hypoxia Maybe through the RhoA–ROCK Signalling Pathway. *Biol. Pharm. Bull.* **2020**, *43*, 432–439. [CrossRef]
12. Li, X.; Luo, X.; Wang, L.; Li, Y.; Xue, M. Acute and subacute toxicity of ethanol extracts from *Salvia przewalskii* Maxim in rodents. *J. Ethnopharmacol.* **2010**, *131*, 110–115. [CrossRef]
13. Dai, D.-S.; Liu, X.; Yang, Y.; Luo, X.-M.; Tang, R.-X.; Yin, Z.-C.; Ren, H.-Q. Protective Effect of *Salvia przewalskii* Extract on Puromycin-Induced Podocyte Injury. *Am. J. Nephrol.* **2015**, *42*, 216–227. [CrossRef]
14. Alsirrag, M.; Ali, R. Determination of antimicrobial and antioxidants activity of *Salvia przewalskii* seed oil against pathogenic bacteria and fungi. *J. Phys. Conf. Ser.* **2018**, *1032*, 012070. [CrossRef]
15. Bolchi, C.; Bavo, F.; Appiani, R.; Roda, G.; Pallavicini, M. 1,4-Benzodioxane, an evergreen, versatile scaffold in medicinal chemistry: A review of its recent applications in drug design. *Eur. J. Med. Chem.* **2020**, *200*, 112419–112435. [CrossRef] [PubMed]
16. Lee, S.R.; Park, Y.J.; Han, Y.B.; Lee, J.C.; Lee, S.L.; Park, H.J.; Lee, H.J.; Kim, K.H. Isoamericanoic Acid B from *Acer tegmentosum* as a Potential Phytoestrogen. *Nutrients* **2018**, *10*, 1915. [CrossRef] [PubMed]
17. Kobayashi, M.; Ueno, H.; Yoshida, N.; Ouchi, H.; Asakawaet, T.; Yoshimura, F.; Inai, M.; Kan, T. Diastereo- and Regiodivergent Total Synthesis of Princepin and Isoprincepin in Both (7″R, 8″R) and (7″S, 8″S) Isomers. *J. Org. Chem.* **2019**, *84*, 14227–14240. [CrossRef]
18. Li, Y.; Xie, S.; Ying, J.; Wei, W.; Gao, K. Chemical Structures of Lignans and Neolignans Isolated from *Lauraceae*. *Molecules* **2018**, *32*, 3164. [CrossRef] [PubMed]
19. Xue, Y.; Wu, Y.; Zhu, H.; Li, X.-N.; Qian, J.-F.; Lai, Y.; Chen, C.; Yao, G.; Luo, Z.; Li, Y.; et al. Salviprzols A and B, C21- and C22-terpenoids from the roots of *Salvia przewalskii* Maxim. *Fitoterapia* **2014**, *99*, 204–210. [CrossRef]
20. Zhu, H.; Chen, C.; Yang, J.; Li, X.-N.; Liu, J.; Sun, B.; Huang, S.-X.; Li, D.; Yao, G.; Luo, Z. Bioactive Acylphloroglucinols with Adamantyl Skeleton from *Hypericum sampsonii*. *Org. Lett.* **2014**, *16*, 6322–6325. [CrossRef]
21. Qiao, Y.; Xu, Q.; Hu, Z.; Li, X.-N.; Xiang, M.; Liu, J.; Huang, J.; Zhu, H.; Wang, J.; Luo, Z. Diterpenoids of the Cassane Type from *Caesalpinia decapetala*. *J. Nat. Prod.* **2016**, *79*, 3134–3142. [CrossRef]
22. Guo, Y.; Zhang, N.; Chen, C.; Huang, J.; Li, X.-N.; Liu, J.; Zhu, H.; Tong, Q.; Zhang, J.; Luo, Z. Tricyclic Polyprenylated Acylphloroglucinols from St John's Wort, *Hypericum perforatum*. *J. Nat. Prod.* **2017**, *80*, 1493–1504. [CrossRef]
23. Wu, Y.; Xie, S.-S.; Hu, Z.-X.; Wu, Z.-D.; Guo, Y.; Zhang, J.-W.; Wang, J.-P.; Xue, Y.-B.; Zhang, Y.-H. Triterpenoids from Whole Plants of *Phyllanthus urinaria*. *Chin. Herb. Med.* **2017**, *9*, 193–196. [CrossRef]
24. Yin, Z.-K.; Liu, Z.-Z.; Yuan, Z.; Feng, Z.-M.; Jiang, J.-S.; Zhang, X.; Zhang, P.-C.; Yang, Y.-N. Thirteen undescribed diterpenoid quinones derived from the rhizomes of *Salvia miltiorrhiza* and their anti-tumor activities. *Phytochemistry* **2021**, *191*, 112902. [CrossRef]

25. Seo, Y.-H.; Trinh, T.-A.; Ryu, S.-M.; Kim, H.-S.; Choi, G.; Moon, B.-C.; Shim, S.-H.; Jang, D.-S.; Lee, D.-H.; Kang, K.-S.; et al. Chemical Constituents from the Aerial Parts of *Elsholtzia ciliata* and Their Protective Activities on Glutamate-Induced HT22 Cell Death. *J. Nat. Prod.* **2020**, *83*, 3149–3155. [CrossRef] [PubMed]
26. Tsai, S.-F.; Lee, S.-F. Neolignans as xanthine oxidase inhibitors from *Hyptis rhomboides*. *Phytochemistry* **2014**, *101*, 121–127. [CrossRef]
27. Yong, H.-C.; Shin, D.; Na, Z.; Lee, H.-S.; Kim, D.-D.; Oh, K.-B.; Shin, J. Dihydroxystyrene Metabolites from an Association of the Sponges *Poecillastra wondoensis* and *Jaspis* sp. *J. Nat. Prod.* **2008**, *71*, 779–783.
28. Lee, D.H.; Cuendet, M.; Vigo, J.S.; Graham, J.G.; Cabieses, F.; Fong, H.H.S.; Pezzuto, J.M.; Kinghorn, A.D. A Novel Cyclooxygenase-Inhibitory Stilbenolignan from the Seeds of *Aiphanes aculeata*. *Org. Lett.* **2001**, *3*, 2169–2171. [CrossRef]
29. Alley, M.C.; Scudiero, D.A.; Monks, A.; Hursey, M.L.; Czerwinski, M.J.; Fine, D.L.; Abbott, B.J.; Mayo, J.G.; Shoemaker, R.H.; Boyd, M.R. Feasibility of drug screening with panels of human tumor cell lines using a microculture tetrazolium assay. *Cancer Res.* **1988**, *48*, 589–601. [PubMed]
30. Chatzopoulou, A.; Karioti, A.; Gousiadou, C.; Lax Vivancos, V.; Kyriazopoulos, P.; Golegou, S.; Skaltsaet, H. Depsides and Other Polar Constituents from *Origanum dictamnus* L. and Their in Vitro Antimicrobial Activity in Clinical Strains. *J. Agric. Food Chem.* **2010**, *58*, 6064–6068. [CrossRef] [PubMed]
31. Kim, G.-D.; Park, Y.-S.; Jin, Y.-H.; Park, C.-S. Production and applications of rosmarinic acid and structurally related compounds. *Appl. Microbiol. Biotechnol.* **2015**, *99*, 2083–2092. [CrossRef] [PubMed]
32. Xu, J.-P.; Wei, K.-H.; Zhang, G.-J.; Lei, L.-J.; Yang, D.-W.; Wang, W.-L.; Han, Q.-H.; Xia, Y.; Bi, Y.-Q.; Yang, M.; et al. Ethnopharmacology, phytochemistry, and pharmacology of Chinese *Salvia* species: A review. *J. Ethnopharmacol.* **2018**, *225*, 18–30. [CrossRef] [PubMed]
33. Wei, W.-J.; Zhou, P.-P.; Lin, C.-J.; Wang, W.-F.; Li, Y.; Gao, K. Diterpenoids from *Salvia miltiorrhiza* and Their Immune-Modulating Activity. *J. Agric. Food Chem.* **2017**, *65*, 5985–5993. [CrossRef] [PubMed]